

## DETERMINING THE SPEED OF A VARIABLE SPEED WIND TURBINE FROM THE VIBRATION RESPONSE

Robert Randall<sup>1</sup>, Michael Coats<sup>2</sup> and Wade Smith<sup>3</sup>

<sup>123</sup>School of Mechanical and Manufacturing Engineering  
UNSW Australia, Sydney NSW 2052, Australia

<sup>1</sup>Email: [b.randall@unsw.edu.au](mailto:b.randall@unsw.edu.au)

<sup>2</sup>Email: [m.coats@yahoo.com.au](mailto:m.coats@yahoo.com.au)

<sup>3</sup>Email: [wade.smith@unsw.edu.au](mailto:wade.smith@unsw.edu.au)

### Abstract

Condition monitoring of wind turbines is very important to minimise maintenance costs (virtually the only costs once they are installed), and to maximise production. New diagnostic techniques have had to be developed to deal with the varying speed and load of the most efficient turbines, but these are greatly aided by having a measure of the speed. This paper shows how the speed of a wind turbine was extracted very accurately from the response vibration signal, making use of a phase demodulation method for determination of a rotational angle vs time map, as used for order tracking. The angle vs time relationship can be determined by the phase demodulation method to any degree of resolution if the corresponding carrier frequency and its sidebands are isolated in the frequency domain with no encroachment from adjacent components. For the case used here for demonstration of the method, the speed range of each signal section had to be limited to about  $\pm 15\%$  to avoid overlap. The overall signal was divided into eight overlapping sections, in each of which a suitable candidate harmonic was isolated, and phase demodulated in two iterations, the second able to use higher harmonics for increased accuracy once separated by the first iteration. Specially designed window functions allowed the results from each section to be smoothly joined. Noise from the differentiation of these phase curves to rotational speed was removed by two methods, which gave very similar results; lowpass filtration in the frequency domain (which however gave some distortion at the two ends) and polynomial curve fitting, which was chosen in this case. The final speed vs time record over the whole record length could then be order tracked using the speed curve itself (integrated to obtain a phase vs time map) to express it as speed vs rotation angle.

### 1. Introduction

Condition monitoring of wind turbines is very important, as the cost of performing maintenance is very high. Even for on-shore turbines, maintenance usually involves the use of expensive cranes, and these cannot operate in strong winds; but wind turbines are usually placed where the winds are strong. Maintenance of offshore wind turbines is even more expensive. Thus it is very important to have advance warning of potential failures so as to be able to avoid them, and in particular the consequential damage which might otherwise multiply repair costs by a very large factor, as well as putting machines out of production for long periods. Condition monitoring of wind turbines is particularly complicated when the rotational speed varies, and the most efficient types now typically vary in speed by up to  $\pm 30\%$ . This can be compensated for if the instantaneous speed is known accurately as a function of time and/or rotational angle, but shaft encoders which give this information are not always mounted.

This paper is based on our group’s contribution to a contest run in connection with the CMMNO (Condition Monitoring of Machines under Nonstationary Operating Conditions) conference held in Lyon, France, in December, 2014. The contest involved making “the most relevant diagnosis of a wind turbine operating under non-stationary conditions” with particular emphasis on two points:

- 1) Diagnosis of a bearing fault on an unspecified shaft
- 2) Determination of the instantaneous speed of the input shaft over the length of the recording

The sponsors of the contest were the French wind turbine manufacturer Maïa Eolis, who provided the signals for analysis, and the French company Oros, who provided the prize, a vibration analysis system.

The indications of the bearing fault in the provided data were very weak, and no contestant made a correct diagnosis. Even the contest organisers had difficulty in providing an indication of the actual fault, which was in a planet bearing in the planetary gear section at entry to the turbine. By applying advanced, but already published, techniques to the bearing diagnostic problem, we did pick up one feature, namely modulation at the speed of the input shaft (the rate at which the faulty bearing was passing the fixed accelerometer), but wrongly ascribed it to a fault in the inner race of the input shaft bearing.

However, the determination of the instantaneous speed required the development of new methods, which are reported in this paper. It also required a complete breakdown of the structure of the vibration signals, to agree with the kinematic information provided, and thus determine the speed (as a fixed ratio of the input speed) of all shafts in the gearbox on which the faulty bearing may have been mounted. This is also described here, although it followed a similar procedure to that presented in [1].

## 2. Background Information

The layout of the turbine gearbox was given by the contest organisers in the following schematic diagram and table. The input was to the planet carrier at the bottom left, and output to the generator at top right.

Gear	Teeth
1	123
2 (3planets)	50
3	21
4	93
5	22
6	120
7	29
8 (not used)	63
9 (not used)	23
10 (not used)	10
11 (not used)	13

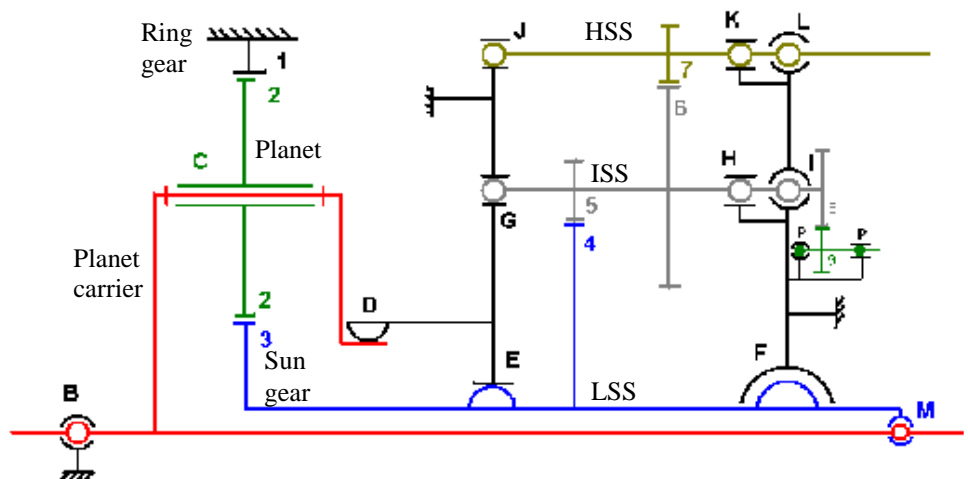


Figure 1. Schematic layout of gearbox components (see Table 1 for LSS, ISS, HSS) Gears indicated by numbers; bearings by letters

From the given data and using standard formulas, the information in Table 1 was calculated for the kinematics of the initial planetary section and the two parallel sections leading to the output. The total speed-up ratio is 119.95, and the order of the output shaft is thus equal to this. It will be seen that this is very close to the order of the planetary gearmesh frequency at 123 (the number of teeth on the ring gear, which are engaged every rotation of the planet carrier).

Table 1 Kinematic details

	Order	tooth nos.
Input (rotor) shaft	1	
Planet carrier	1	
Planetary section		
Ring gear, Z1		123
Planet gears (3), Z2		50
Sun gear, Z3		21
Sun gear shaft (LSS)	6.8571	
Gearmesh (PGM)	123	
First parallel section		
LSS, Z4		93
ISS, Z5		22
Intermediate shaft (ISS)	28.987	
Gearmesh (IGM)	637.71	
Second parallel section		
ISS, Z6		120
HSS, Z7		29
High speed shaft (HSS)	119.95	
Gearmesh (HGM)	3478.4	

### 3. Analysis of the Gear Train

The signal was first analysed as a spectrogram, to see how the various spectral components changed with time along the record. This is shown in Figure 2, in a full bandwidth version and one decimated by a factor of 5 to emphasise the lower frequency regions up to 500 Hz. Speed information had to be extracted from the signal itself, using speed related components with as little interference as possible from adjacent components and noise. From Fig. 2(b) it is seen that there are two potential candidates, one centred on about 50 Hz, most likely the second harmonic of output shaft speed (HSS), or planet gearmesh frequency (PGM), and the other centred on about 280 Hz, most likely the second harmonic of the intermediate gearmesh frequency (IGM). These average frequencies would correspond to an input speed of about 13 rpm (0.22 Hz).

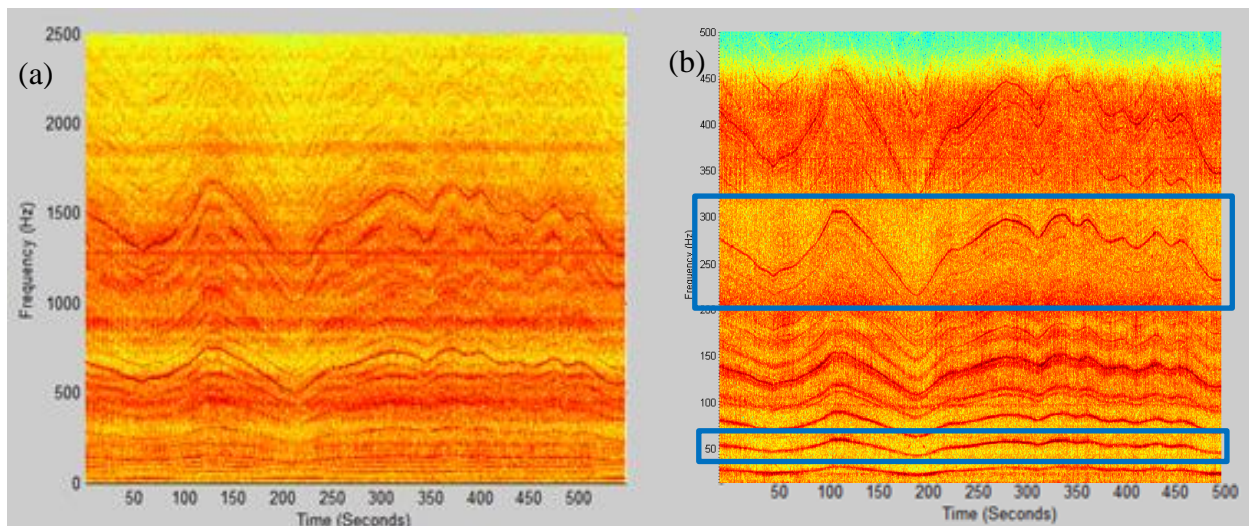


Figure 2. (a) Full bandwidth spectrogram (b) Spectrogram to 500 Hz, with two separated components

For this initial analysis, a continuous record of reasonably constant speed (from 250-500s) was analysed to find the relationships between the basic spectral components. It is necessary to perform an “order analysis”, to remove the effects of varying speed and present the “frequency spectra” on a harmonic order rather than an actual frequency axis. This is the same as converting the time axis to one



of revolutions (of a reference shaft), and means resampling the time signals to a fixed number of samples per revolution and preferably with a known starting phase with respect to the position of this shaft. This process is called order tracking, and can be achieved in different ways. A shaft encoder giving a fixed number of pulses per rev can be used to sample the signal directly, but then all information is lost about time. In “computed order tracking” (COT) a shaft encoder or tacho signal is recorded at the same time as other signals to be tracked, and used to produce a phase (rotation angle) vs time map, which can then be used to resample the signals at times corresponding to equal phase increments.

A very efficient COT method uses phase demodulation to generate the phase/time map; this has the advantage that as long as the demodulated frequency band is not contaminated by overlapping components from adjacent carriers, or other sources, the phase/time relationship can be obtained to any degree of resolution by appropriate oversampling. This approach is described in detail in [2], which explains that even with a pure reference signal, eg from a tachometer, overlap of modulation sidebands can occur if the speed changes by a given amount (max.  $\pm 33\%$  for the fundamental order, and less for higher orders and/or higher sweep rates). This is discussed later.

Under some conditions, the reference frequency can be a response component rather than a tacho or shaft encoder signal. The basic requirement is that the response time of the system should be small with respect to the time taken to change speed appreciably. This is discussed in detail by Borghesani et al. in [3]. Because of their huge inertia, wind turbines usually do not represent a problem in this respect.

Figure 3 shows the results of analysis of the most stable section of signal, including the spectrum zoomed around 55 Hz, which was phase demodulated to perform the order tracking, using the method of reference [2]. Figure 3(a) shows that the component near 55 Hz is well separated from adjacent components, and this was used for the first stage demodulation. It was actually the second harmonic of the planetary gearmesh frequency (PGM), which meant that the allowable maximum speed variation to avoid overlapping of sidebands would have been  $< \pm 15\%$ . As can be inferred from Fig. 3(b) the first harmonic of PGM was not clearly separated from the background. A second iteration was performed, using the second harmonic of intermediate gearmesh frequency (IGM), and Fig. 3(b) shows the resulting order spectrum. The low harmonics are shown below to be dominated by the planetary gearmesh frequency (PGM), while the higher ones are confirmed to be harmonics of the IGM. Spectrograms were drawn of the order tracked signal, in both frequency ranges, confirming that orders were now horizontal lines, but there is not room to include them.

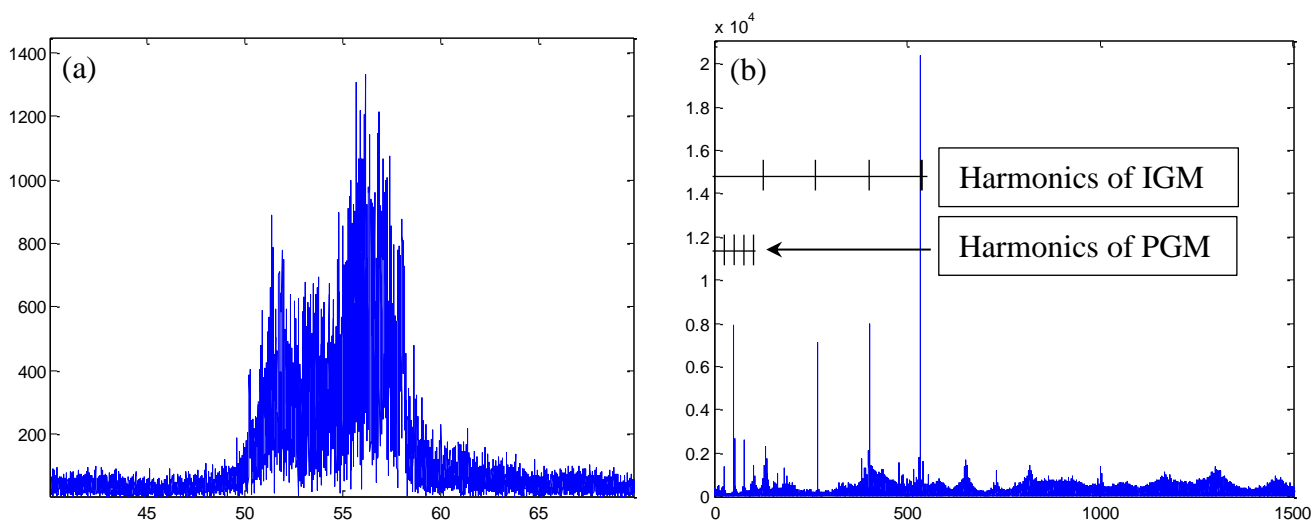


Figure 3. (a) Component near 55 Hz, used for first iteration (b) Order tracked spectrum

Partly because of the proximity of the PGM and the HSS, there was some difficulty to establish the latter, but it was achieved using a finely tuneable harmonic cursor. Zooming on the very low portion of Fig. 3(b) in Fig. 4, it can be seen that the 123<sup>rd</sup> harmonic of the input speed is confirmed to be the PGM (every 3<sup>rd</sup> input harmonic strong because it is the planet pass, and blade pass, frequency). This is shown in Figure 4(a). The apparent output shaft speed (HSS) is very close to Harmonic 120. Placing a

harmonic cursor on this identified HSS component, gives a 29<sup>th</sup> harmonic corresponding to the high speed gearmesh frequency (HGM). This is shown in Fig. 4(b). Note the sidebands around HGM, which will be shown to be spaced at ISS. Two points should be noted: (a) Nominal frequency axes of order tracked spectra can be disregarded; the harmonic cursors show the order relationships, and (b) the smearing of the low frequency components in Fig. 4(a) is presumably because the order tracking was based on the IGM (with an order > 600 times the input speed) and the ratio is likely smeared by the elasticity of the gear train.

The two sets of harmonic cursors in Fig. 5 show that the HGM is both 29×HSS and 120×ISS, and that the sideband spacing is at ISS. Correspondence of the ISS harmonic series is particularly clear at 4×IGM (88×ISS). Thus, it can be assumed that the various components of the order tracked spectra have been identified and confirmed as conforming with the given data.

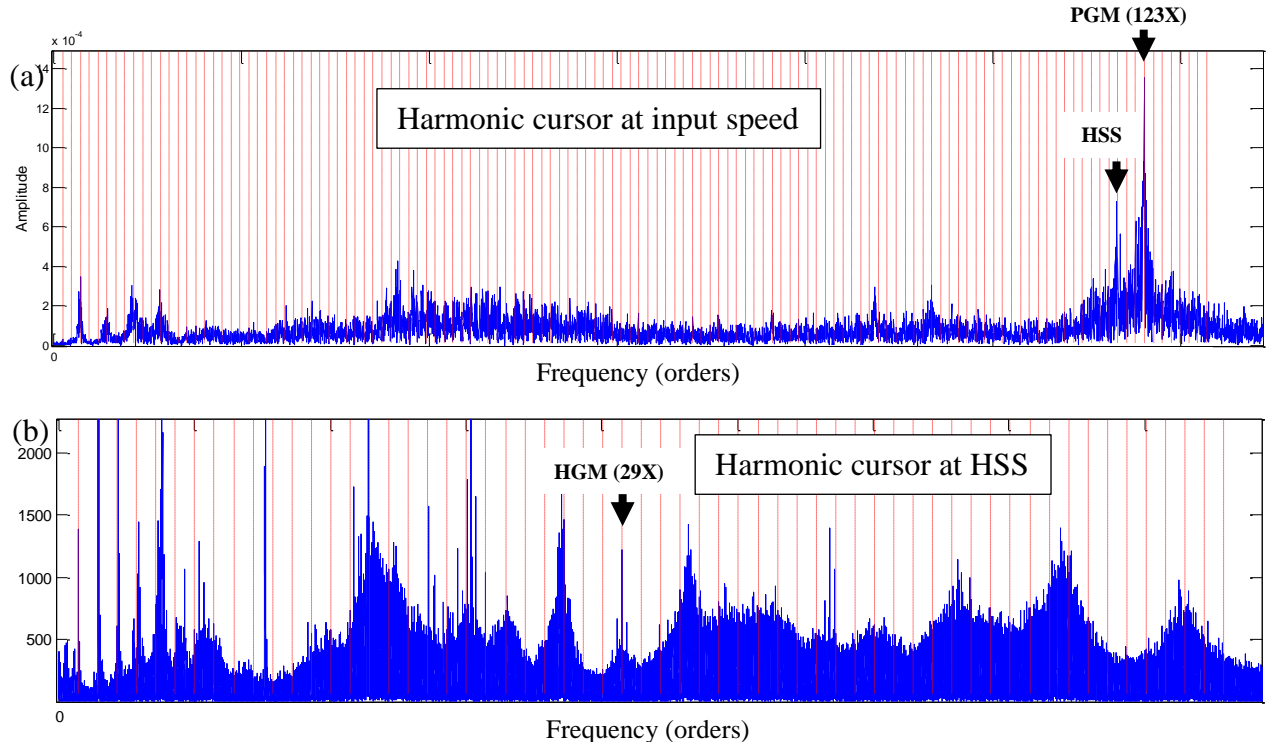


Figure 4 Identification of PGM, HSS and HGM from input shaft speed

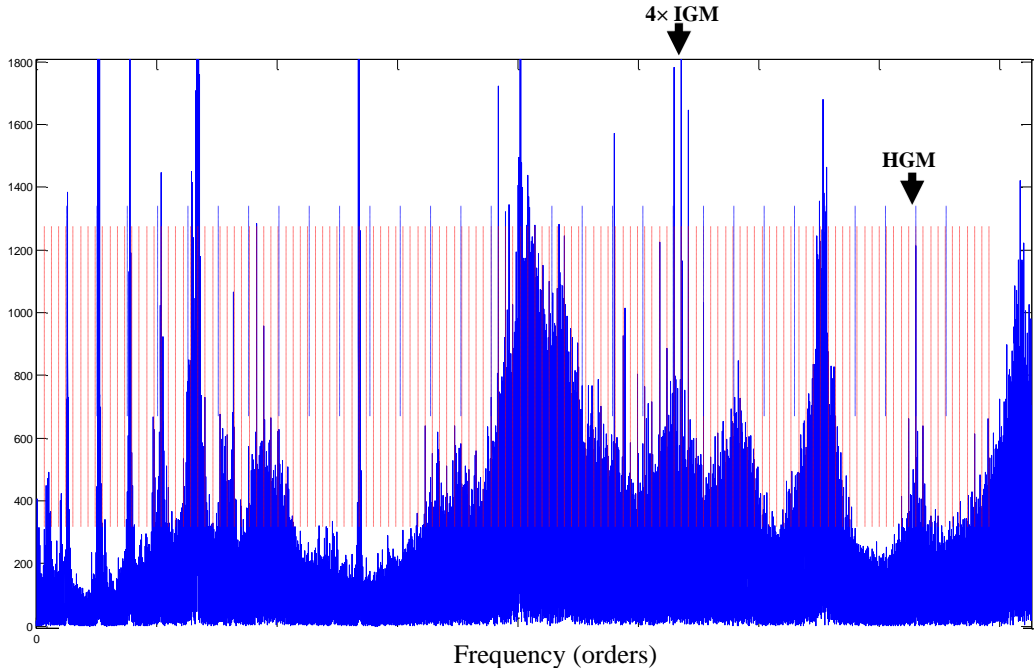


Figure 5. Demonstrating that HGM is both 29×HSS and 120×ISS

## 4. Determination of Output Shaft Speed

Because of the speed variation outside the section just analysed (250s – 500s), it was necessary to use a different approach for determination of the instantaneous speed. The problem of using the phase demodulation method for order tracking of a signal with speed variation greater than that otherwise allowable had already been solved for cases such as machine run-ups and run-downs, as presented in [4]. It consists in dividing the record up into overlapping segments, in each of which the speed variation is within the limits. In the overlapping regions, the signals are windowed by weighting functions tapering from 1 (one) to zero, and such that the overlapping window functions add to unity at each point in time. A typical choice of window function is the “half Hanning” as illustrated in Figure 6, for a couple of adjacent segments. A full Hanning window is of course a raised cosine (or cosine squared) function over one period of the sinusoidal part. The length of the half cosines has to be the same for the overlapping part of two adjacent segments, but not necessarily at either end of the same segment. Even though the change of x-axis from time to rotation angle distorts the shape of the window, it does not change the fact that they add to unity at every point even after resampling. Individual segments, after order tracking, can be re-joined by simple addition. It is convenient to make the breakpoints, where the adjacent windows each have value 0.5, initially half way across the overlap area, the point where the phase of adjacent segments is aligned. Note that in the order tracking process, as explained in [4], the initial value of phase at the start of each record is somewhat arbitrary, but can be adjusted to be continuous along the whole record after order tracking.

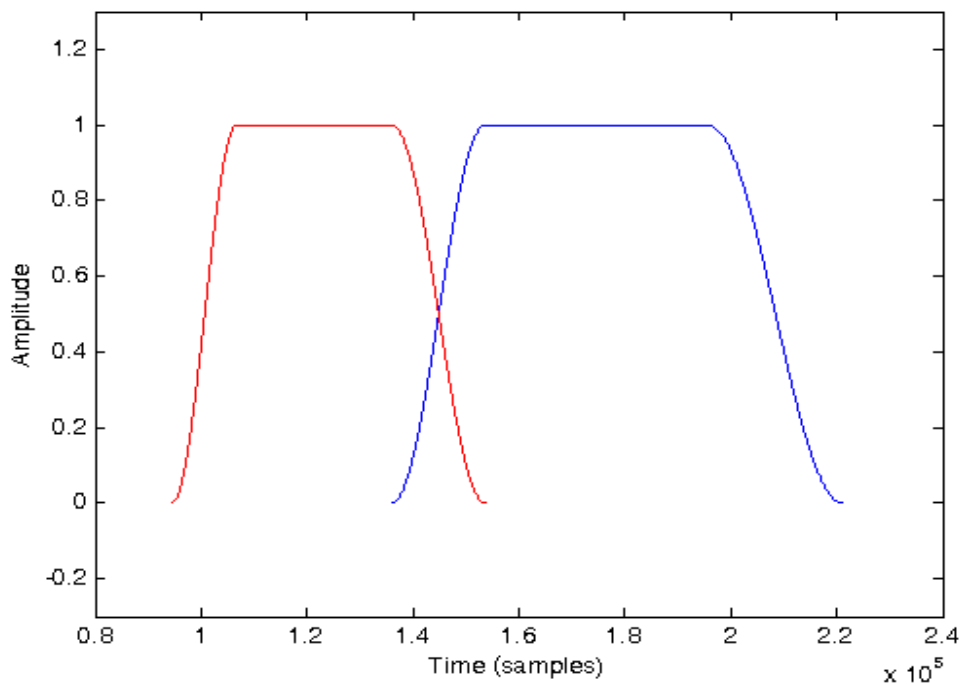


Figure 6. Half Hanning windows applied to adjacent segments, adding to unity in the overlap area

In the current case, it was found by inspection that the signal could be divided into eight overlapping segments, with break points every 50s, to 300s, then a 200s long segment to 500s, followed by another short segment just less than 50s until the end of the record. These segments were chosen so that at least one harmonic order was reasonably isolated in the frequency domain (as for the second harmonic of PGM in Fig. 3(a)). The best choice for all these segments was found to be the third harmonic of PGM, and this was used to obtain a map of phase (rotation angle) vs time to allow determination of its derivative, the angular speed. Since only low frequency information was required (speed of the output shaft), the signal decimated by 5 to a sampling frequency of 1 kHz (with appropriate lowpass filtering) was processed. Because of the considerable slope of these phase curves, and the need to match up the phase both at and around the break points if they were to be joined, it was decided to attempt instead to obtain the instantaneous speed in each segment, by differentiation of the phase, as this should be continuous and more uniform along the record. The differentiation greatly increased the noise at high

frequency (multiplication by  $j\omega$ ), but it was thought that this noise could be eliminated by smoothing. Two methods were used for the smoothing:

- (1) Blending of the overlapped segments (2.5s on either side of each break point) by cosine tapering of the *differences* between the two curves (Figure 7(b)), followed by lowpass filtering of the combined record in the frequency domain.
- (2) Polynomial curve fitting of each segment, and then blending the individual segments in the overlap areas by the same cosine tapering process.

Figure 7 shows the overlapping individual segments, and the result of combining them (before lowpass filtering). The y-axis is scaled in arbitrary units but 0.5 corresponds to an output speed of 26 Hz. This scaling carries over to Fig. 8, but Fig. 9 is scaled correctly in terms of the output speed in Hz.

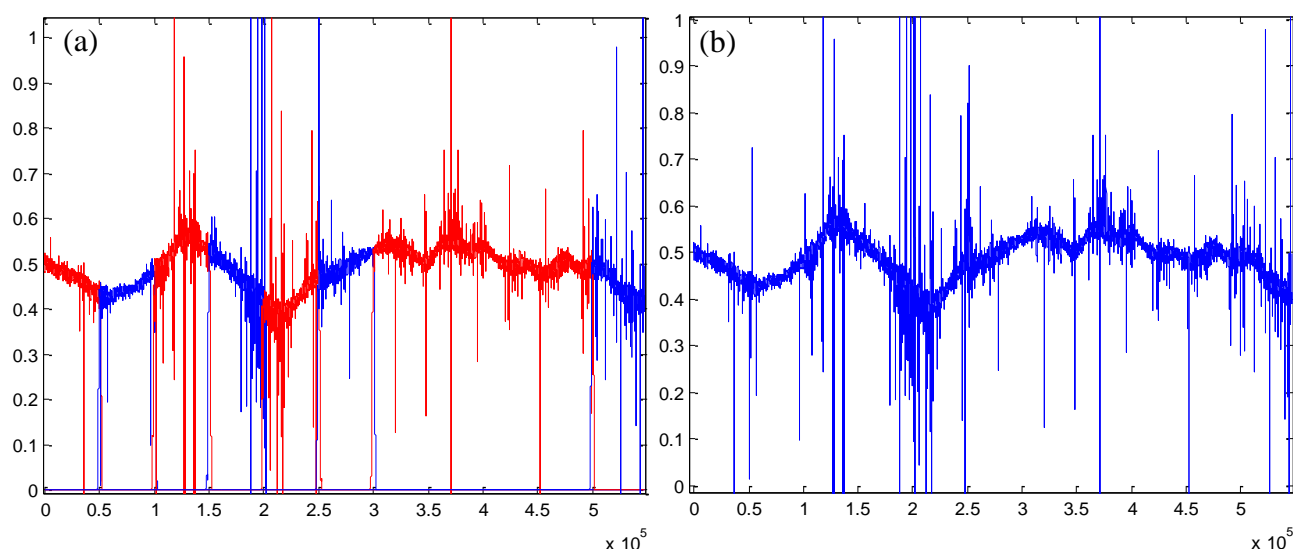


Figure 7. (a) Compilation of the 8 overlapping segments (b) Result of blending by cosine tapering

Despite the apparent noisiness of the curves, both smoothing methods gave good results. Figure 8(a) shows the result (in red) of curve fitting (with a polynomial of order 20) on the long section from 300-500s. Order 5 was found satisfactory for the shorter sections. Figure 8(b) compares the final results by the two methods, which are very similar to each other, and to the typical components in the spectrogram of Fig. 1(b), in particular the second harmonic of IGM between 200-300 Hz. Though there is little difference between them, the LP filtered curve is possibly slightly more correct, but with wraparound errors at the two ends because of the circularity of FFT processing. The polynomial fitted version was thus chosen for further processing, because the final desired resolution (8 samples per revolution of the output shaft) required even further smoothing.

The speed curve was scaled to the first order of the output shaft in Hz, and order tracked using a phase map obtained by integration (Matlab “Cumsum”) of the speed curve itself. Fig. 9(a) compares the two curves. It was initially resampled to 24 samples per rev (similar to the existing sample rate) and then decimated to 8 samples per rev in a final step (as requested by the contest organisers). This curve is depicted in Figure 9(b). It will be noted that according to these results the input shaft speed did vary up to 15 rpm, as stated in the contest document, but down to less than 11 rpm (rather than 13 rpm as stated in the contest document). This range seems to be confirmed by the spectrograms of Fig. 1.

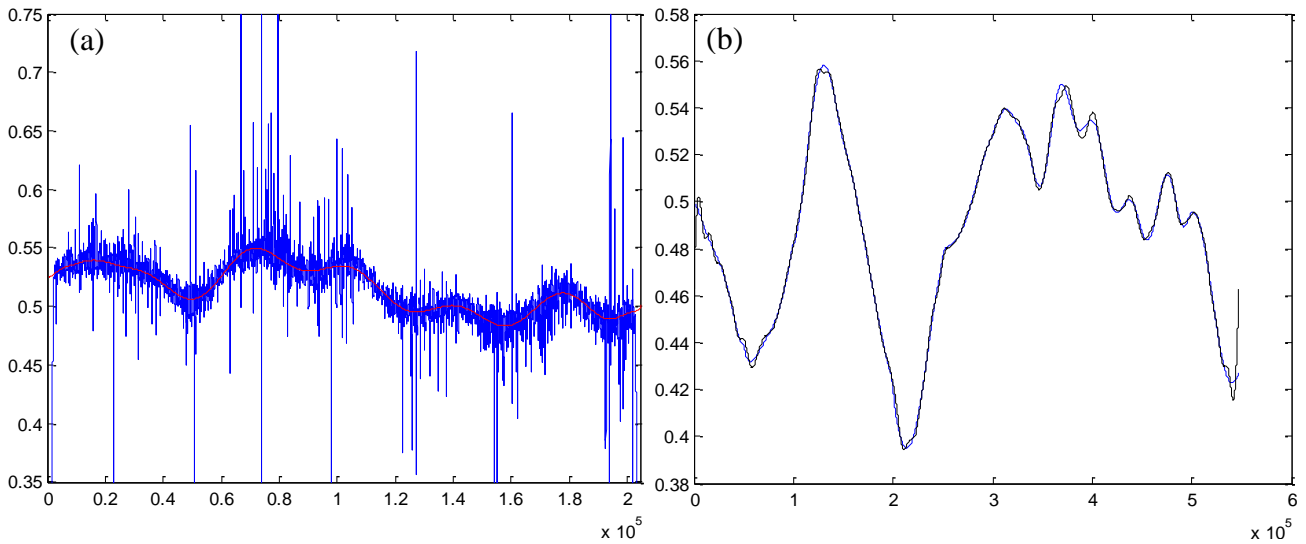


Figure 8. (a) Polynomial (order 20) curve fit of segment 7  
 (b) Comparison of Polyfit (blue) and LP filter (black)

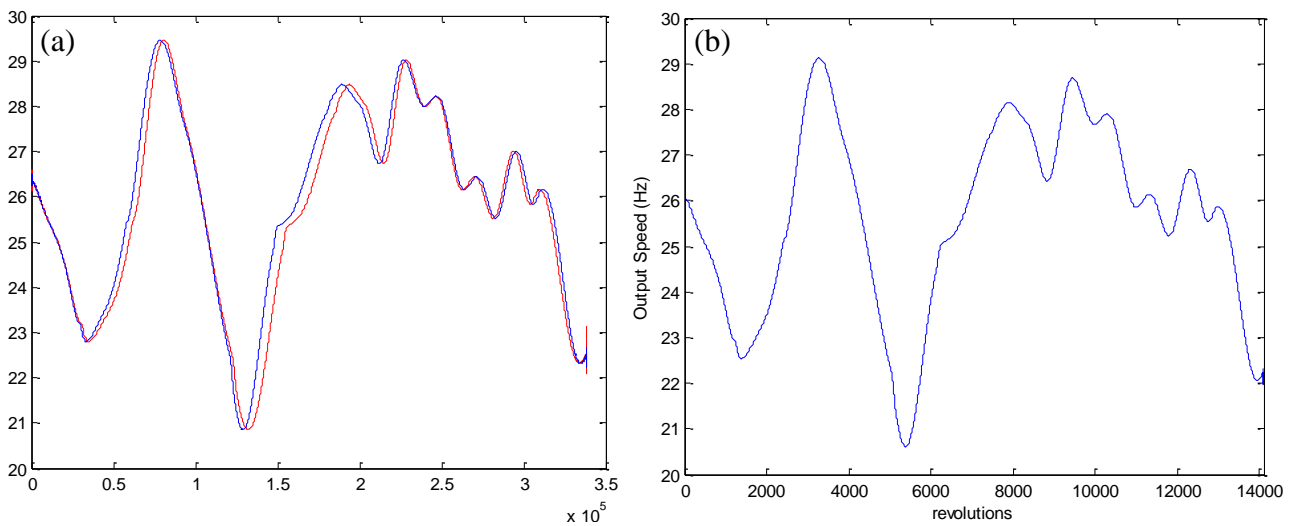


Figure 9. (a) Speed (Hz) vs (red) time (blue) rotation; (b) Speed vs rotation, 8 samples/rev

#### 4.1 Outcome

Our group was awarded the prize for the closest entry to the measured tachometer signal [5]. The results of the three closest contestants are compared with the tachometer in Figure 10. This gives a strong indication that the method is valid in fairly general circumstances. It is worth noting that where our result deviates most from the tachometer (130-150 and 370-410 “seconds”) the lowpass filtered result is somewhat closer (Fig. 8(b)). It is perhaps also worth noting that because of the elasticity of the gear train itself, a tachometer mounted on the high speed output shaft (as here) might not give exactly the same result as a tachometer mounted on the low speed input shaft. This points to the possibility that even if a tachometer is used for the first iteration, to remove most of the speed variation and give the possibility of accessing higher harmonics of all shafts for later iterations, it might be possible to optimise the actual speed estimate separately for the low, intermediate and high speed sections of the gearbox, by demodulating the harmonics of shafts in each section.



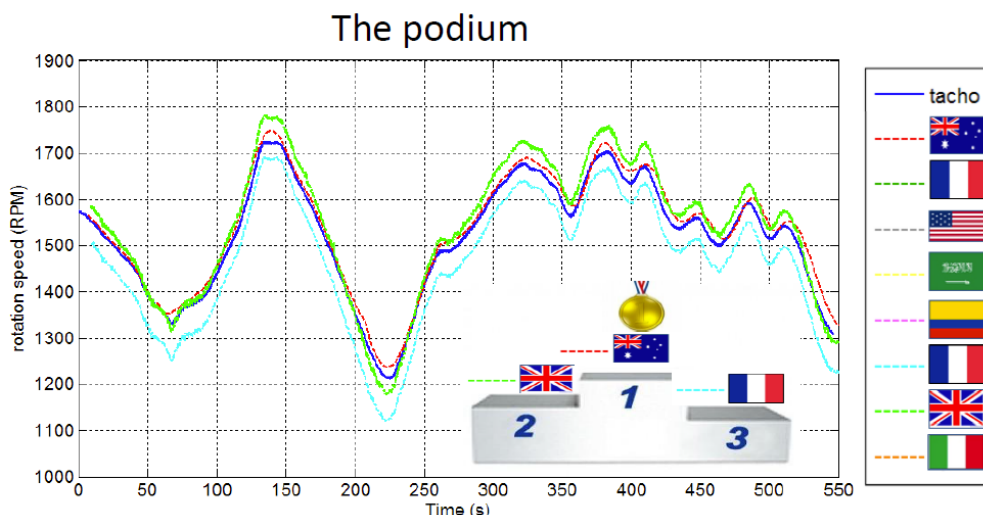


Figure 10. Comparison of the results of the three top entries

## 6. Conclusions

Diagnostic methods are now available for machines with variable speed, such as wind turbines, but they depend on knowing the instantaneous speed so as to be able to compensate for it. It has been shown that it is possible to extract the speed information from the signal itself as long as at least one speed related harmonic is isolated in the frequency domain from adjacent components. This will often be a dominant first harmonic, as this is maximally separated from the next (the second) but even so, the maximum speed variation without overlap of sidebands around these two harmonics is about  $\pm 30\%$ , and correspondingly less for higher harmonics. If the speed varies outside these limits the signal can be divided into overlapping segments in each of which the speed variation is within the limits, and the speed determined by phase/frequency demodulation seamlessly joined in the overlapping sections.

The example given in the paper is taken from a contest to make a diagnosis of a wind turbine gearbox operating with variable speed. The kinematics of the gearbox was first confirmed by order tracking a section with  $< \pm 15\%$  variation, first using the second harmonic of the planetary gearmesh frequency (PGM), followed by a second iteration based on the second harmonic of the intermediate gearmesh frequency (IGM). These were both found from an initial spectrogram to be well separated from adjacent components.

For determination of the speed, the signal was divided up into eight sections in each of which the speed variation was  $< \pm 10\%$ , allowing the third harmonic of IGM to be demodulated to determine the phase vs time. This was then differentiated to frequency (angular velocity) which was expected to be continuous in adjacent sections. The differentiation introduced additional high frequency noise, but this was easily removed by two methods of smoothing. One used lowpass filtration in the frequency domain, which gave wraparound errors at the two ends of the record, and the other used polynomial curve fitting, which avoided this problem, but probably lost some fine detail. The speed vs time curve was integrated to give phase vs time, which could then be used to express the speed as a function of rotation angle rather than time, as requested by the contest organisers. The results based on polynomial curve fitting were submitted and gave the best results in a contest from a field of eight entries. It is perhaps worth mentioning however that the method based on lowpass filtration would probably be better if the end effects can be mitigated (possibly by simply using a slightly longer record and discarding the two ends, which was not possible for this contest).

## Acknowledgements

This research was supported by the Australian Research Council and SpectraQuest, through Linkage Project LP110200738. The authors are grateful to the contest sponsors Maïa Eolis and Oros, for allowing the contest data and results to be used in a publication.

## References

- [1] Sawalhi N. and Randall R.B., “Gear parameter identification in a wind turbine gearbox using vibration signals”, *Mechanical Systems and Signal Processing*, **42**(1-2), 368-376, (2014).
- [2] Coats, M.D. and Randall R.B., “Single and multi-stage phase demodulation based order-tracking”, *Mechanical Systems and Signal Processing*, **44**(1-2), 86-117, (2014).
- [3] Borghesani, P., Pennacchi, P., Randall, R.B., Ricci, R., “Order tracking for discrete-random separation in variable speed conditions”, *Mechanical Systems and Signal Processing*, **30**, 1–22, (2012).
- [4] Coats, M.D. and Randall R.B., “Order tracking under run-up and run-down conditions”, *Proceedings of IFTOMM Rotor Dynamics*, Milan, September, (2014).
- [5] André, H. and Leclère, Q. “CMMNO Industrial Contest Results”. (Accessed 12/08/2015). <http://cmmno2014.sciencesconf.org/conference/cmmno2014/pages/PresentationCMMNOcontestwopicts.pdf>